Integrated adsorption-ORC system:

Al-Mousawi, Fadhel; Al-Dadah, Raya; Mahmoud, Saad

Link to publication on Research at Birmingham portal

1
2
Integrated adsorption-ORC system: Comparative study of four scenarios to generate cooling and power simultaneously

3 **Fadhel Noraldeen Al-Mousawi[a,b*], Raya Al-Dadah[a], Saad Mahmoud[a]**

4 [a] Department of Mechanical Engineering, University of Birmingham, United Kingdom, B15 2TT, United Kingdom

5 [b] Department of Mechanical Engineering, University of Karbala, Karbala, Iraq

6 [*] e-mail address: fna397@bham.ac.uk (fadhelnor@gmail.com)

7 **Abstract**

8 Adsorption cooling and Organic Rankine Cycle (ORC) systems are promising technologies that can
9 be used to exploit the abundant amount of low grade heat sources such as solar energy, geothermal
10 energy and waste heat from industrial processes. In this study, a two bed adsorption cooling cycle has
11 been integrated with an ORC to simultaneously generate cooling and power utilising AQSOA-ZO2
12 (SAPO-34)/water and silica-gel/water as adsorption working pairs and R245fa, R365mfc and R141b
13 as ORC working fluids. Four different scenarios of integrated adsorption-ORC system have been
14 investigated, where in the first three scenarios, adsorption system is set up as a topping system, while
15 ORC is set up as a bottoming system. The first one utilized the waste heat of adsorption to power the
16 ORC system with no additional heat and named as Adsorption Heat Recovery Scenario (AHRS). In
17 the second scenario the adsorption return heating fluid is used to power the ORC system (Return
18 Adsorption Heating Fluid Scenario RAHFS). In the third scenario (Heat Exchanger Scenario HES),
19 the cooling and heating sources leaving the adsorption system enter a heat exchanger, where
20 additional heat can be added to the cooling fluid in order to power the ORC system. In the fourth
21 scenario (Return ORC Heating Fluid Scenario RORCHFS), the ORC is considered to be as a topping
22 system, while the adsorption system considered as bottoming system and the return ORC heating fluid
23 can be used to power the adsorption cycle. Results show that when using AHRS, the integrated
24 adsorption -ORC system can achieved system efficiency of 70% using silica-gel/water and R141b and
25 60% using SAPO-34/water and R141b. In addition, the maximum Specific Power (SP) and Specific
26 Cooling Power (SCP) can be achieved utilising SAPO-34 and R141b with values of 208 W/kg$_{ads}$ and
27 616 W/kg$_{ads}$ respectively. This work highlights the potential of using integrated adsorption cooling
28 system and ORC to generate cooling and power simultaneously.

29 **Keywords** Adsorption, ORC, Cooling and power generation, AQSOA-Z02 (SAPO-34), Silica-gel

30

Nomenclature

Symbols		ρ	density kg/m^3
A	adsorption potential, J/mole	φ	flag
A$_r$	area, m^2	**Subscript**	
c_p	specific heat capacity, J/kg.K	ads,a	adsorbent
k$_o$	empirical constant in Eq. (6), 1/s	ads	adsorption
E$_a$	activation energy, J/kg	bed	adsorbent bed
H	enthalpy, J/kg	chill	chilled water
H$_{fg}$	evaporation latent heat J/kg	des	desorption
M	mass, kg	eff	effective
$\dot{m}$	mass flow rate, kg/s	evap	evaporator
P	pressure, Pa	f	liquid
Q$_{st}$	isosteric heat of adsorption, J/kg	g	gas
R	gas constant, J/kg.K	i	adsorption/desorption
R$_p$	adsorbent practice radius, m	in	inlet
U	overall heat transfer coff., W/m^{2}K	j	cooling / heating source
W	power generated W	o	outlet
SP	specific power generated W/kg$_{ads}$	ref	refrigerant
SCP	specific cooling power W/kg$_{ads}$	r	ratio
t	time, s	s	saturation
T	temperature, K	cond	condenser
x	adsorption uptake, kg/kg$_{ads}$	w	water
x$_{eq}$	equilibrium uptake, kg/kg$_{ads}$		

1. Introduction

As population has grown significantly during last century, millions of people who live in developing

countries still lack to access to secure electricity grids and the problem becomes worse in hot

countries where a large amount of power is needed for air conditioning. In addition, using

conventional fossil fuels has a negative impact on the environment issue such as global warming and

the climate change which pushed more research towards a real change in the energy policy [1].

Organic Rankine cycle (ORC) used in a range of applications, including industrial waste heat

recovery [2], solar thermal [3], biomass power plants [4], and geothermal [5]. Table (1) demonstrates

a number literature using ORC with a range of working fluids and heat source temperatures.

Table 1: Organic Rankine cycle (ORC).

Author	Working fluid	Evap. Temp. ^{o}C	ORC type	Results
Le et al [6]	R134a, R152a R32, R744, R1270, R290, R1234yf, R1234ze(E)	150	Supercritical (basic and regenerative)	Max efficiency of 13.1% using R152a
Pei et al [7]	R-123	120	Regenerative	Max efficiency of 8.6%, 9.2% higher than basic efficiency
Mago et al [8]	R113, R245ca, R123, and isobutane	100-210	Regenerative	Higher first and second efficiencies than basic efficiency and lower irreversibility
Aljundi [9]	12 refrigerants	50–140	Basic with heat exchanger	Max efficiency of 13.36% using neo-Pentane
Tchanche et al [10]	20 refrigerants	60–100	Solar with heat storage	R134a appears as the most suitable for small scale solar applications
Roy et al [11]	R12, HCFC-123, HFC-134a, R717	277 (heat source)	non-regenerative	R-123 produces the maximum efficiencies and output with minimum irreversibility

Absorption and adsorption cooling systems utilising low grade heat sources have the advantage of

being environmentally friendly. A number of researchers investigated the absorption cooling

technology experimentally [12] and numerically [13], while many researchers investigated means of

improving the adsorption cooling technology including different adsorption system configurations

[14][15][16], various working pairs [17][18] through modelling[19][20] and experimental work [21].

However, ORC systems are capable to utilize a range of low grade heat sources and generate

electricity, it shows relatively low efficiency compared to similar low grade heat utilization

technologies like adsorption. In addition, air conditioning usually consumes a large amount of

48 electricity especially in hot countries, so it would be more practical to convert the low grade heat into

49 cooling and electricity directly and simultaneously to enhance the overall system efficiency and

50 reduce the energy conversion losses. Table (2) demonstrate a number of literature that use a range of

51 technologies to generate cooling and power at the same time.

Table 2: Technologies used for cooling and power generation.

Absorption technology			
Author	Working pair/fluid	Source temp. ^{o}C	System performance
Vijayaraghavan, and Goswami [22]	Ammonia/water	87-207	Cycle efficiency increased by 25%.
Hasan et al [23]	Ammonia/water	57-197	Maximum second law efficiency of 65.8%
Liu and Zhang [24]	Ammonia/water	450	18.2% reduction in energy consumption.
Zheng et al [25]	Ammonia/water	350	Thermal and exergy efficiency of 24.2% and 37.3%.
Zhang and Lior [26]	Ammonia/water	450	Thermal and exergy efficiencies of 27.7%, and 55.7%.
Adsorption technology			
Author	Working pair/fluid	Source temp. ^{o}C	System performance
Lu et al [27]	12 different salts /ammonia	100-200	40%-60% increase in exergy efficiency compared with Goswami cycle.
Jiang et al [28]	5 different salts/ammonia	100-400	Thermal efficiency of 15.8%, COP of 0.691 and exergy efficiency of 82%.
Wang et al [29]	$PbCl_2$/ ammonia $BaCl_2$/ ammonia $CaCl_2$/ ammonia	100-400	Exergy efficiency improved by 40-60%
Bao et al [30]	$MnCl_2$/ammonia	150-210	0.57 COP and 62% exergy efficiency
Bao et al [31]	$CaCl_2$/ammonia	120-130	490 W of power and 5.4 ^{o}C of chilled water
Jiang et al [32]	MnCl2-CaCl2-NH3	130	300 W of power and 2 kW of cooling and efficiency increases from 31.6% to 37.6%.
Lu et al [33]	12 different salts/ammonia	100-300	COP increased by 38%, electricity efficiency improved from 8% to 12% and second law efficiency reached 41%.
AL-Mousawi et al [34]	MIL101Cr/water	70-90	Cycle efficiency increased from 47% to 50%
AL-Mousawi et al [35]	AQSOA-Z02/water MIL101Cr/water Aluminium-Fumarate/water silica-gel/water	80-160	Small-scale radial inflow turbine of 82% efficiency was designed and modelled using SAPO-34 and total system efficiency of 69% can be achieved.
AL-Mousawi et al [36]	AQSOA-Z02/water MIL101Cr/water silica-gel/water	80-160	SP of 73 W/kg$_{ads}$, and SCP of 681 W/kg$_{ads}$ using AQSOA-Z02 and maximum system efficiency of 67% can be achieved.
Adsorption technology and ORC			
Author	Working pair/fluid	Source temp. ^{o}C	System performance
Jiang et al [37]	$CaCl_2$/$BaCl_2$ and R245fa	< 100	Energy and exergy efficiencies were 10.1%-13.1% and 18.5%-20.3
Wang et al [38]	silica-gel/water and R600	78 -98	1 kW of electricity and 6.3 kW of refrigeration from 15 kW of heat

52 A number of researchers [22-26] have investigated the production of cooling and power using

53 absorption technology, however this technology has a number of negatives like large size, and toxicity

54 of ammonia. Production of cooling and power using adsorption technology was investigated by a

55 number of researchers [27-36], via incorporating an expander in such system, however, this

56 configuration may have a limited amount of power generation due to the relatively low refrigerant

57 mass flow rate passing through the expander (coming from the desorber) especially when small

58 amount of adsorbent is used.

59 Adsorption is an exothermic process and cooling source is needed during this process to

60 sustain the cooling in the evaporator and during this process heat is rejected in the bed that

61 undertaking the adsorption process. Heat recovery is one of the best proposed ways to benefit

62 from the internal thermal energy of the adsorption cooling system itself, and improving the

63 overall system's performance. In this point, researchers have put forward some effective

64 means that promotes a useful use of the internal heat of the system. Wang et al. [39]

65 experimentally studied the effect of passive heat recovery on the coefficient of performance

66 and results show that the COPs of a two-bed chiller and a four-bed chiller have improved by

67 as much as 38% and 25%, respectively, without any effect on their cooling capacities. Pan et

68 al. [40] studied and compared the theoretical analysis of three heat recovery methods used in

69 adsorption refrigeration system and results show that serial and passive heat recoveries (part

70 type) are more optimal than circular heat recovery (complete type) when manufacture and

71 cost are considered. Leong et al. [41] studied numerically the effect of using combined heat

72 and mass recovery in adsorption cooling cycle and results show that the proposed cycle can

73 increase the coefficient of performance (COP) of an adsorption cooling system by more than

74 47% compared to the single bed system. However, all the previous work does not cover the

75 use of rejected heat from adsorption process to power another cycle like Organic Rankine

76 cycle, while, some researchers [37][38] used the heat source leaving the ORC system to

77 power the adsorption system, but again nobody used the cooling source (with heat recovery)

78 that leaving the adsorption as a heat source for an ORC system and not all the possible

79   scenarios of integrating the adsorption system with ORC to generate cooling and power

80   simultaneously were investigated, so there is still a clear gap of using adsorption cycle as a

81   topping system, while ORC as a bottoming system, where ORC can be totally or partially

82   powered using the heat recovered from the adsorption system which helps to enhance the

83   overall system efficiency.

84   In this paper a two bed cooling adsorption system has been integrated with an ORC using four

85   different scenarios to investigate the feasibility of generating cooling and power simultaneously

86   utilising low grade heat sources. The system comprises of two adsorption beds, two condensers and

87   two evaporators and an expander (turbine) using AQSOA-Z02 (SAPO-34)/water and silica-gel/water

88   as adsorption pairs and R245fa, R365mfc and R141b as ORC working fluids.

89   1. **Integrated ORC-adsorption system**

90   Figure (1a) shows a schematic diagram of a basic two-bed adsorption cooling system which consists

91   of desorber, adsorber, condenser and evaporator As the adsorption is an exothermic process a cooling

92   source is used to extract heat from the adsorber and sustain cooling through adsorption process which

93   helps to desorb the refrigerant from the evaporator and generate the cooling effect. Desorption is an

94   endothermic process, and a heat source (low grade heat source) is used to sustain heating during this

95   process which helps to discharge the refrigerant (water vapour) from the hot bed. Then, the hot

96   refrigerant will be cooled in the condenser to feed the evaporator with the refrigerant liquid and keep

97   continuous cooling through the system. Figure (1b) shows the adsorption basic cycle on a P-T

98   diagram; process 1-2 is an adsorbent isosteric heating where a low grade heat source is used and this

99   heating is still continuous during the process 2-3' while the valve 4 is opened, meanwhile a cold

100   source is used during the process 3'-4' and this cooling is still continuous during the process 4'-1

101   while the valve 2 is opened.

102

(a)   (b)
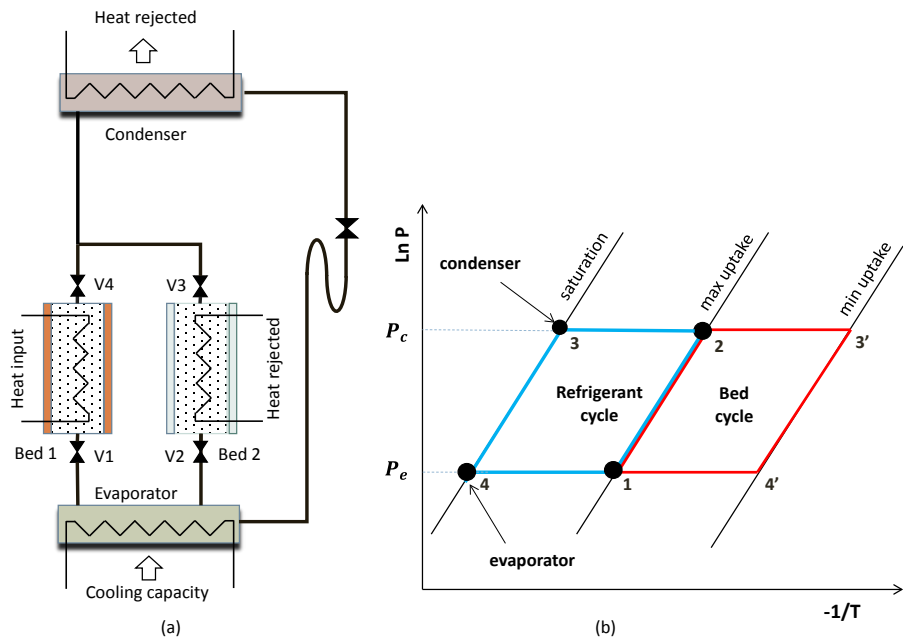
Figure 1: shows a basic two-bed adsorption cooling (a) schematic diagram (b) P-T diagram.

The basic Organic Rankine cycle (ORC) as shown in Figure (2) can be powered by a low grade heat sources such as solar energy or waste heat and it has four main processes. During process 1-2 the refrigerant liquid will be pumped to the evaporator pressure, while through process 2-3 heat is added to the evaporator from an external source (low grade heat source). During, 3-4 the refrigerant expands through an expander (turbine) where the mechanical power can be produced and finally, through 4-1 the refrigerant is cooled in the condenser.

(a)   (b)
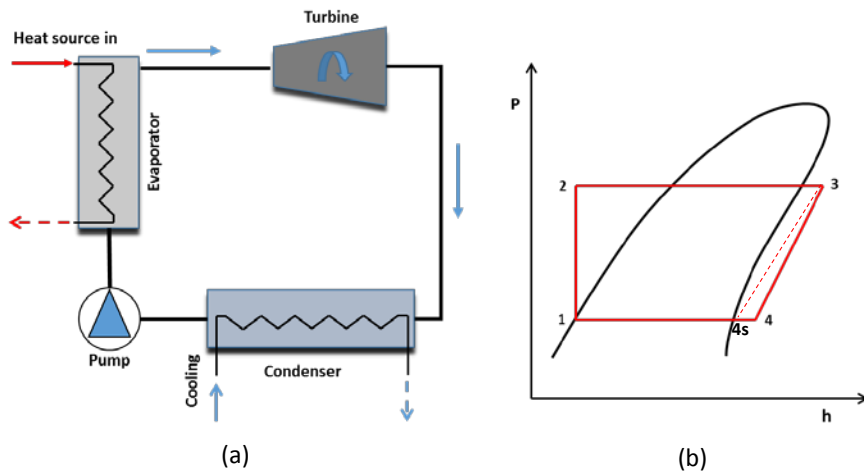
Figure 2: Basic ORC cycle (a) schematic diagram (b) P-h diagram.

6

115　The main purpose of this study is to investigate the feasibility of producing cooling and power

116　simultaneously by modifying the two-bed adsorption system to be integrated with an ORC system and

117　improve the heat utilization efficiency. This study can be carried out using four proposal scenarios as

118　listed below.

119　　a)　Adsorption Heat Recovery Scenario (AHRS): in this scenario, the two bed adsorption

120　　　　cooling system is powered using an external low grade heat source such as solar energy or

121　　　　geothermal energy to sustain the desorption process in the hot bed. While, during the

122　　　　adsorption process (in the cold bed) adsorption material needs to be cooled using an

123　　　　external cooling source to release the heat of adsorption and sustain the adsorption

124　　　　process and as a result it sustains the cooling effect in the evaporator which is one of the

125　　　　main outputs of the integrated system. In this scenario, the heat of adsorption can be

126　　　　recovered by the cooling source fluid and as the cooling source inlet temperature is

127　　　　relatively high (but still enough to cool the bed under adsorption process), the cooling

128　　　　source leaving the bed can be used to power an Organic Rankine cycle and generate

129　　　　electricity without using additional heat. Figure (3) shows the two bed adsorption system

130　　　　integrated with an ORC system to generate cooling and power simultaneously, where the

131　　　　adsorption cooling system is used as topping system and the ORC is used as bottoming

132　　　　system and during this scenario all valves are closed except V6 and V7 as listed in table

133　　　　(3).

134　　b)　Return Adsorption Heating Fluid Scenario (RAHFS): in this scenario, the cooling system

135　　　　is powered using an external low grade heat source such as solar energy or geothermal

136　　　　energy to sustain desorption process in the hot bed, while a cooling source is used to

137　　　　sustain the adsorption process. The adsorption cooling system is used as topping system

138　　　　and ORC is used as bottoming system and in this case ORC system is powered using the

139　　　　same low grade heat source line leaving the hot bed in the adsorption cooling system

140　　　　(topping system), so additional heat can consumed by the ORC system and more

141　　　　electricity is expected to be generated using this scenario and this is due to using

142   relatively high driving temperature to power the ORC system. Figure (3) shows the two

143   bed adsorption system integrated with an ORC system to generate cooling and power

144   simultaneously, where the ORC (bottoming system) is powered using the hot line (water

145   or pressurized water depends on the heat source temperature) leaving the adsorption

146   system (topping system) and during this scenario all valves are closed except V5 and V8

147   as shown in table (3).

148   c) Heat Exchanger Scenario (HES): in this scenario, the adsorption cooling system is

149   powered by an external low grade heat source to drive the hot bed during desorption

150   process, while a cooling source is used in the cold bed. This scenario is similar to AHRS,

151   where again the cooling source line recovers the heat of adsorption from the cold bed

152   during adsorption process. This recovered heat can be partially used to power an Organic

153   Rankine cycle and generate electricity, where additional heat from the external heat

154   source is added in this scenario (by using additional heat exchanger) to enhance the

155   efficiency of the ORC system. Figure (3) shows that the hot line (water or pressurized

156   water) and the cold line leaving the adsorption system enter a heat exchanger to add

157   additional amount of heat from the hot line to the leaving cold line, so this heat (the

158   recovered heat and the additional heat) is used to power the ORC system and in this

159   scenario, all valves are open except V8 as shown in table (3).

160   d) Return ORC Heating Fluid Scenario (RORCHFS): in this scenario, the ORC system is

161   used as the topping system while the adsorption cooling system is used as the bottoming

162   system and an external low grade heat source is used to power the ORC system. The

163   heating fluid leaving the ORC system is used directly to power the two bed adsorption

164   system and as results, the integrated system (of adsorption system and ORC system) can

165   generate cooling and power at the same time. Figure (4) shows the integration of ORC

166   and adsorption cooling system using this scenario.
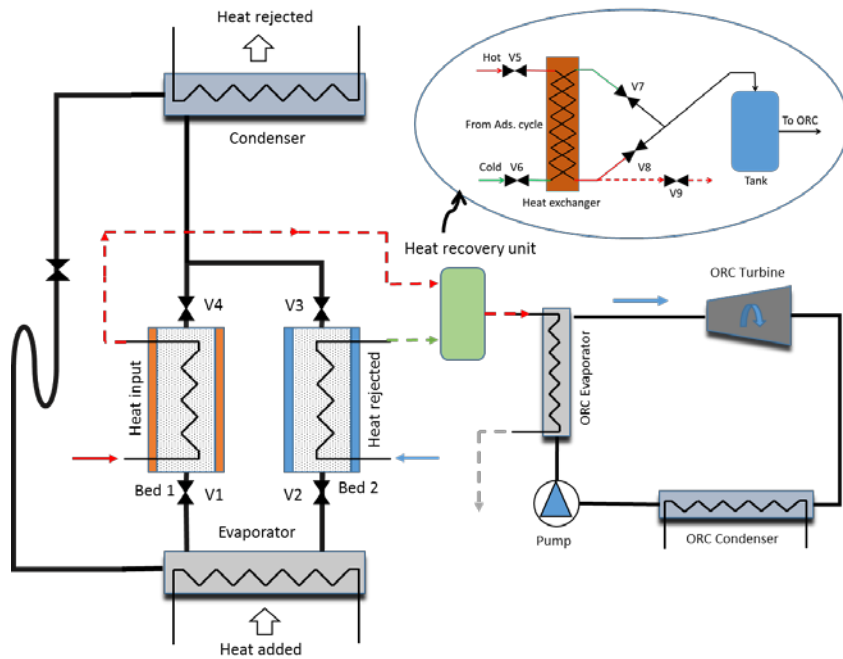
167

168

Table 3: Scenarios AHRS, RAHFS and HES valves situation.

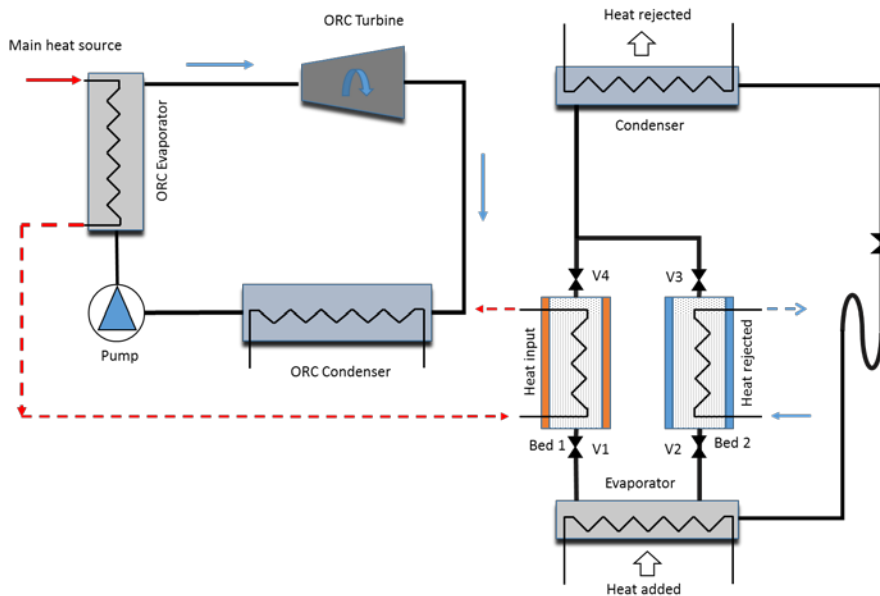| Scenario	V5	V6	V7	V8	V9
AHRS	C	O	O	C	C
RAHFS	O	C	C	O	C
HES	O	O	O	C	O

169

170

171   **Figure 3: Schematic diagram of an adsorption –ORC integrated system scenarios 1, 2 and 3.**


172

173   **Figure 4: Schematic diagram of an adsorption –ORC integrated system scenarios 4.**

174

175

2. Adsorbent materials properties

In this study AQSOA-Z02 (SAPO-34) is used and compared to silica-gel and this material is considered to be an advanced (synthetic zeolite) with a unique adsorbent performance that has been developed by MITSUBISHI PLASTIC Company using inorganic material design technology. Figure (5a) shows scanning electron microscope SEM image of AQSOA-Z02 which has solid regular cubic or brick shape with a uniform particle and it has smaller particle size compared to silica-gel. Figure (5b) shows the AQSOA-Z02 structure where, it has pore size of 0.38 nm compared to the water molecule size of 0.3 nm.
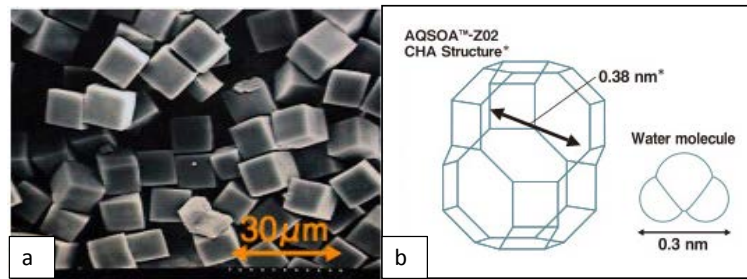
Figure 5: (a) SEM image for AQSOA Z02, and (b)CHA structure for AQSOA Z02 [42].

Figure (6) shows the measured isotherms of AQSOA-Z02 (SAPO-34)/water (experimental data from a DVS analyser) at three temperatures (25 °C, 35 °C and 45 °C) and the corresponding curve fitting lines [36]. In this figure, the experimental data is fitted to the equation that developed by Sun and Chakraborty [43] (equation 1) and a good agreement is obtained between the experimental data (dotted lines) and the predicted data (continuous lines) at all temperatures (25 °C, 35 °C and 45 °C) with maximum deviation of about ±12%. The constants obtained from this fitting are listed in table (4), while the equation is given by:
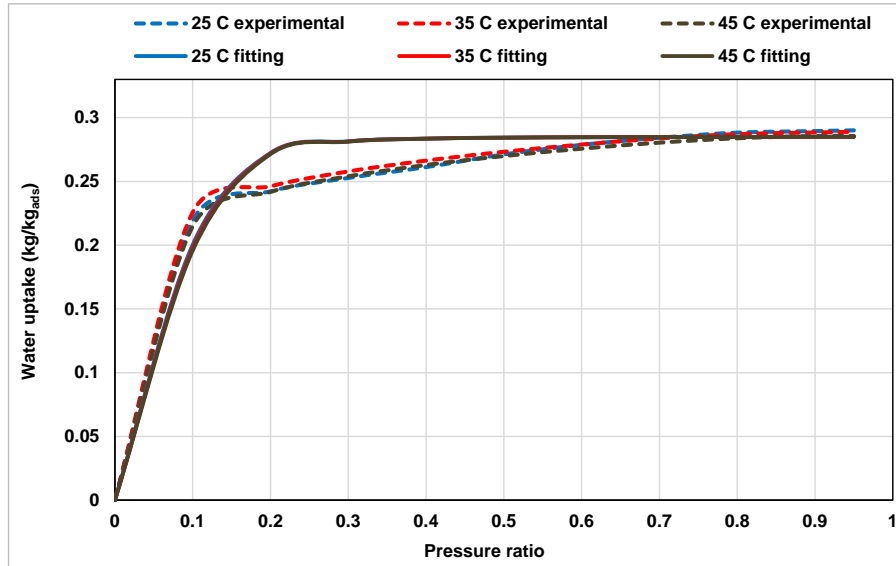
$$x_{eq} = x_o \left[\frac{k(\frac{p}{p_s})^n}{1+(K-1)(\frac{p}{p_s})^n} \right] \tag{1}$$

$$k = \alpha exp\left[n(Q_{st} - h_{fg})/RT\right] \tag{2}$$

10

Table 4: Constants used in Equations (1) and (2) [36].

Property	Value	Unit
x_o	0.285	kg/kg$_{ads}$
α	1032	-
n	3.18	-
Q_{st}	3420	kJ/kg

196

197

198   **Figure 6: Isotherms fitting of experimental and predicted uptake of AQSOA Z02 (SPO-34)/water[36].**

199   The modified Freundlich equation is used to present the adsorption isotherms of silica-gel/water

200   [44][45][46] as:

201    $$x_{eq} = A(T_s)\left[\frac{p}{p_s}\right]^{B(T_s)} \tag{3}$$

202   Where

203    $$A(T_s) = A_o + A_1 T_s + A_2 T_s^2 + A_3 T_s^3 \tag{4}$$

204    $$B(T_s) = B_o + B_1 T_s + B_2 T_s^2 + B_3 T_s^3 \tag{5}$$

205   The constants of equations (4) and (5) are obtained from [46][47]. Adsorption and desorption is a time

206   dependant process and are assumed to be controlled by macroscopic diffusion and the linear driving

207   force (LDF) equation is used to define the adsorption/desorption rate as [44][45][48]

208    $$\frac{dx}{dt} = k_o exp(-E_a/RT)(x_{eq} - x) \tag{6}$$

11

209   For AQSOA-Z02 (SAPO-34)/water, the kinetics constants of equation (6) are obtained from [49],

210   while for silica-gel/water the values of kinetics constants used in equation (6) are : k_o= 1.3183 E+05

211   1/s and E_a= 42000 J/mole [44][45].

212   **3. Integrated system energy balance**

213   The lumped model technique is used to describe the energy balance equations in the two adsorbent

214   beds used in this study, where the adsorbent, the refrigerant and the bed materials are assumed to be at

215   the same temperature at all time of the cycle[48][50][51].

216

$$\left(Mc_{p_{eff}}^{bed}\right)\frac{dT^{bed}}{dt} + \left(M_a x_i^{bed} c_p\right)\frac{dT_i^{bed}}{dt} = \varphi M_a \left(\frac{dx_i^{bed}}{dt}\right)(Q_{st}) - (\dot{m}c_p)_j \left(T_{j,o} - T_{j,in}\right) \quad (7)$$

217   Flag φ equals to 0 at switching time and equals to 1 at adsorption/desorption process. The first term

218   on the left side of the equation (7) shows the internal energy change in heat exchanger material,

219   including the fins and the tubes, while the second term represents the change in internal energy of the

220   refrigerant (water). The first term on the right side of equation (7) represents the heat

221   generated/rejected during the adsorption/desorption process respectively. The last term describes heat

222   added/rejected to the coolant during the adsorption/desorption process and the bed outlet temperature

223   is given by: [48][50]

224

$$T_{j,o} = T_i^{bed} + \left(T_{j,in} - T_i^{bed}\right)\exp\left[\frac{-(UA_r)_i^{bed}}{(\dot{m}c_p)_j}\right] \quad (8)$$

225   The energy balance equations for the condenser can be expressed by [51][52]

226

$$\left(Mc_{p_{eff}}^{cond}\right)\frac{dT^{cond}}{dt} = \varphi H_{fg} M_a \frac{dx_{des}^{bed}}{dt} - (\dot{m}c_p)_{cond}\left(T_{w,o} - T_{w,i}\right) - (c_p)_w (T^{bed} - T^{cond}) M_a \frac{dx_{des}^{bed}}{dt} \quad (9)$$

227   The condenser outlet temperature is given by [51][52]

228

$$T_{w,o} = T^{cond} + \left(T_{w,in} - T^{cond}\right)\exp\left[\frac{-(UA_r)^{cond}}{(\dot{m}c_p)_{cond}}\right] \quad (10)$$

229   The energy balance in the evaporator is expressed as [51][52]

230 $$\left(Mc_{p_{eff}}^{evap}\right)\frac{dT^{evap}}{dt} = \varphi H_{fg}M_a\frac{dx_{ads}^{bed}}{dt} - (\dot{m}c_p)_{evap}\left(T_{chill,o} - T_{chill,i}\right) - (c_p)_w(T^{cond} - T^{evap})M_a\frac{dx_{des}^{bed}}{dt} \quad (11)$$

231 The outlet temperature of the chilled water can be written as [45][52][51]

232 $$T_{chill,o} = T^{evap} + \left(T_{chill,in} - T^{evap}\right)exp\left[\frac{-(UA_r)^{evap}}{(\dot{m}c_p)_{evap}}\right] \quad (12)$$

233 The mass balance of liquid refrigerant in the adsorption evaporator is given as [45][48][50][51]

234 $$\frac{dM_{ref}}{dt} = -M_a\left[\frac{dx_{des}^{bed}}{dt} + \frac{dx_{ads}^{bed}}{dt}\right] \quad (13)$$

235 Heat added to the ORC evaporator (Q_{in}) and heat rejected in the ORC condenser (Q_{out}) can be
236 written as [53][54][55] :

237 $$Q_{in} = \dot{m}_{e,orc}c_p(T_{e,i} - T_{e,o}) \quad (14)$$

238 $$Q_{out} = \dot{m}_{c,orc}c_p(T_{c,i} - T_{c,o}) \quad (15)$$

239 In equation (14), $\dot{m}_{e,orc}$ is the mass flow rate of heating fluid (water or pressurized water) passing

240 through the ORC evaporator which equals to the bed cooling fluid (water) mass flow in AHRS and

241 HES, the bed heating fluid mass flow in RAHFS and to the main heat source mass flow in

242 RORCHFS. $T_{e,i}$ is the inlet temperature of ORC evaporator which equals to cooling fluid leaving the

243 hot bed in AHRS, the heating fluid leaving the hot bed in RAHFS, the cooling fluid leaving the cold

244 bed and the heat exchanger in HES and the main heat source temperature in RORCHFS, while $T_{e,o}$ is

245 temperature of the fluid leaving the ORC evaporator. In equation (15), $\dot{m}_{c,orc}$ is the mass flow rate of

246 the cooling fluid (water) using to cool the ORC condenser which is constant during this study as

247 shown in table (5), while $T_{c,i}$ and $T_{c,o}$ are the inlet and the outlet cooling fluid temperatures of the ORC

248 condenser and as shown in figures (2-4) the isentropic efficiency of the ORC turbine can be given by:

249 $$\eta_T = \frac{h_3 - h_4}{h_3 - h_{4s}} \quad (16)$$

250 The power generated by the ORC turbine can be calculated as:

251 $$W_{turbine} = \eta_{turbine}\dot{m}_{ORC}(h_3 - h_4) \quad (17)$$

252 The ORC cycle thermal efficiency can be calculated as:

253 $\quad \eta_{ORC} = \frac{W_{turbine}-W_{pump}}{Q_{in}}$ $\qquad$ (18)

254 The power consumed in pump can be calculated as:

255 $\quad W_{pump} = \frac{\dot{m}_{ORC}(P2-P1)}{\rho_1 \eta_{pump}}$ $\qquad$ (19)

256 The overall performance of the integrated system is evaluated using the specific cooling power (SCP),

257 specific generated power (SP), the cooling coefficient of performance (COP) and overall system

258 efficiency as expressed in equations (20-23).

259 $\quad SCP = \frac{(\dot{m}c_p)_{evap} \int_0^{t_{cycle}}(T_{chill,o}-T_{chill,i})dt}{M_a t_{cycle}}$ $\qquad$ (20)

260 $\quad SP = \frac{\int_0^{t_{cycle}} \dot{m}_{ORC}(h_3-h_4)dt}{M_a t_{cycle}}$ $\qquad$ (21)

261 $\quad COP = \frac{(\dot{m}c_p)_{evap} \int_0^{t_{cycle}}(T_{chill,o}-T_{chill,i})dt}{(\dot{m}c_p)_h \int_0^{t_{cycle}}(T_{h,o}-T_{h,i})dt}$ $\qquad$ (22)

262 $\quad system\ efficiency = \frac{(\dot{m}c_p)_{evap} \int_0^{t_{cycle}}(T_{chill,o}-T_{chill,i})dt + \int_0^{t_{cycle}} \dot{m}_{ORC}(h_3-h_4)dt}{(\dot{m}c_p)_h \int_0^{t_{cycle}}(T_{h,o}-T_{h,i})dt}$ $\qquad$ (23)

263   4. **System modelling**

264 MATLAB Simulink software is used to simulate the integration a two bed adsorption system

265 with an ORC system to study the feasibility of generating cooling and electricity

266 simultaneously. The main components of the adsorption system such as beds, condenser and

267 evaporator in addition to the ORC system are presented in a flow chart as shown in figure (7)

268 to highlight the main steps used to solve the system equations (1-23).

Figure 7: System modelling flow chart.
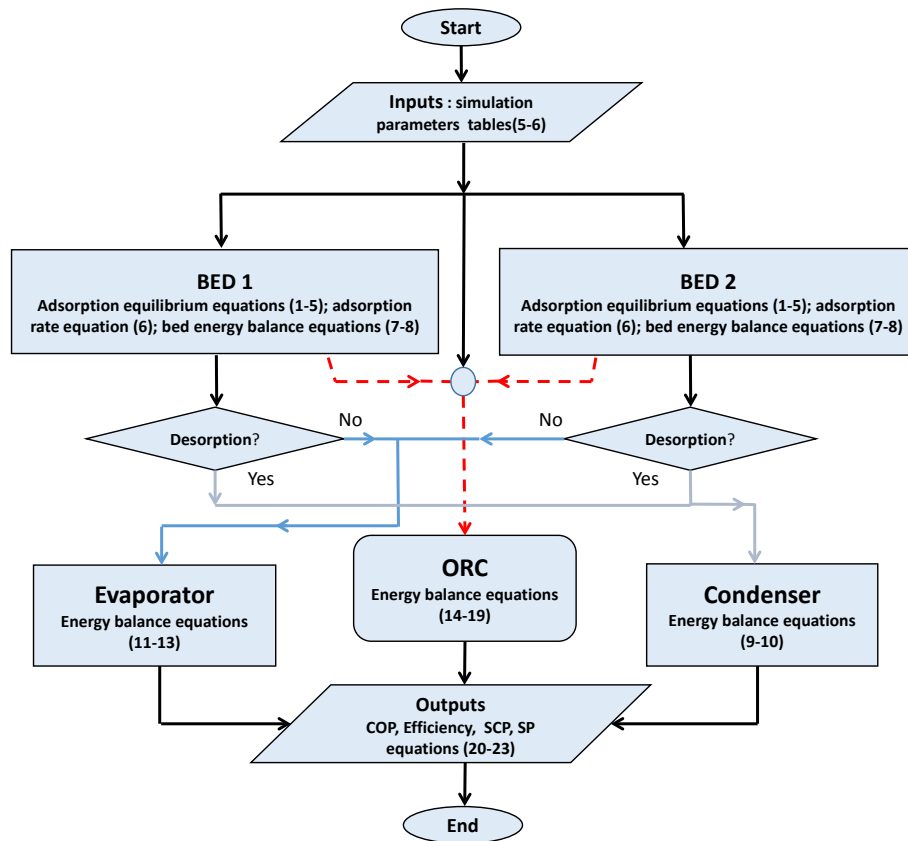
5. Results and discussion

Table (5) shows the main operating conditions where the same conditions were applied for all scenarios except the cold bed temperature (48 ^{o}C for AHRS and HES) and the ORC condenser temperature (25 ^{o}C for AHRS and HES), while table (6) shows the characteristics of main components used in this study. Figure (8) shows the output of the adsorption-ORC integration system for cooling and power using AQSOA-Z02 (SAPO-34)/water as a working fluid and utilising heat source temperatures of 95 ^{o}C. The cycle can produce average cooling and power of up to 2.73 kW (using RAHFS) and 1.17 kW (using RORCHFS and R141b) respectively. Figure (9) compares the COP of adsorption cooling system and the efficiencies of ORC system and integrated adsorption-ORC system for the four proposed scenarios using a range of heat source temperatures utilising silica-gel/water as adsorption pair and R245fa, R365mfc and R141b as ORC fluids. Results show that, AHRS has the maximum integrated system efficiency of about 70% and this is because no additional heat is used in this scenario and ORC is powered only by the heat recovered from

15

adsorption cycle. Also HES has relatively high overall efficiencies compared to RAHFS and

RORCHFS because HES is similar to AHRS, with a limited amount of additional heat that

used through the heat exchanger. Figure (10) presents similar data but, using AQSOA Z02

(SAPO-34)/water as adsorption pair and again AHRS shows the highest integrated system

efficiency of 60%,while HES has relatively high overall efficiencies compared to RAHFS

and RORCHFS and this is for the same reason as for silica-gel/water. Figure (11) shows the

SCP and SP of the integrated adsorption-ORC system for the four proposed scenarios

utilising silica-gel/water and R245fa, R365mfc and R141b. Results show that, AHRS and

HES show the lowest value of SCP due to using relatively high cooling source temperature

and the lowest value of SP due to the relatively low pressure ratio through the ORC turbine

caused by low temperature in the ORC evaporator. RAHFS shows the highest SCP of almost

432 W/kg$_{ads}$ using silica-gel because adsorption system is the topping system where more

heat is applied to the adsorption beds. RORCHFS shows the highest SP of almost 169

W/kg$_{ads}$ using silica-gel and R141b with heat source temperature of 115 ^{o}C and this is due to

ORC is topping system and more heat is added to the ORC evaporator in this scenario. Figure

(12) presents similar data but, for AQSOA Z02(SAPO-34)/water and results show that

RAHFS shows the highest SCP of almost 616 W/kg$_{ads}$ and RORCHFS shows the maximum

SP of 208 W/kg$_{ads}$ using R141b and heat source temperature of 115 ^{o}C.

The four different scenarios used in this investigation can offer a range of options not only to

the designers of energy systems, but also to the energy consumers. For example, in hot

countries, air conditioning and refrigeration are considered to be the largest portion of the

total residential energy consumption, and the proposed integrated system can be used as

localized units to generate cooling and electricity simultaneously especially in the remote or

off-grid areas (areas which are not connected to the national or main electricity grid), also this

helps to increase the overall utilization efficiency of the low grade heat sources. AHRS is

preferable when limited amount of low grade heat source is available because this scenario can generate cooling and electricity simultaneously with high efficiency. Even though, RAHFS and RORCHFS can generate cooling and power at the same time with relatively high SP and SCP, the efficiencies of those scenarios are low compared to the efficiencies of AHRS and HES. However, if the used low grade heat source is infinite or semi-infinite like solar energy (as in many hot countries around the world) those scenarios can be more preferable. In addition, in this study energy losses through turbine and pump are considered where the efficiencies of the turbine and the pump are assumed to be 85% and 65% respectively as listed in table (5), while the energy losses through heat exchangers, pipes, and valves are neglected, because they are expected to be thermally insulated.

Table 5: Parameters used in the simulation.

Parameter	Value
Bed heating fluid temperature ^{o}C	95-115
Bed cooling fluid temperature ^{o}C	48^a/30
Condenser cooling temperature ^{o}C	30
Chilled water temperature ^{o}C	14
Bed hot fluid mass flow rate kg/s	1.7
Bed cold fluid mass flow rate kg/s	1.6
Condenser mass flow rate kg/s	0.75
Evaporator mass flow rate kg/s	0.75
Half cycle time s	320
Switching time s	20
ORC condenser temperature ^{o}C	25^a/30
ORC condenser mass flow kg/s	0.8
ORC refrigerant mass flow kg/s	0.04
Expander (turbine) efficiency %	85
Pump efficiency %	65

321

322

323 **Table 6: System characteristics** [36][56]**.**

324 **(a) Bed heat exchanger characteristics**

Parameter	Value
Fin length m	172E-3
Fin width m	30E-3
Fin pitch m	1.2E-3
Module length m	450E-3
No. of module	4
No. tubes/module	6
Tube OD m	15.875E-3
Tube thickness m	0.8E-3

325 **(b) Adsorption condenser/evaporator characteristics**

Parameter	Value
Pipe length m	5.5
No. tubes	4
Tube OD m	15.875E-3
Tube thickness m	0.8E-3

326 **(c) ORC condenser/evaporator characteristics**

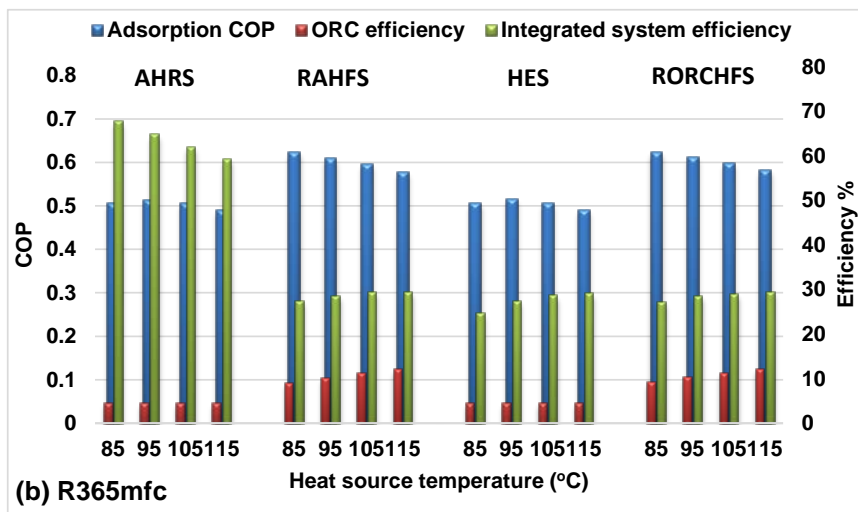| Parameter	Value
Pipe length m	5.5
No. tubes	8
Tube OD m	15.875E-3
Tube thickness m	0.8E-3

327
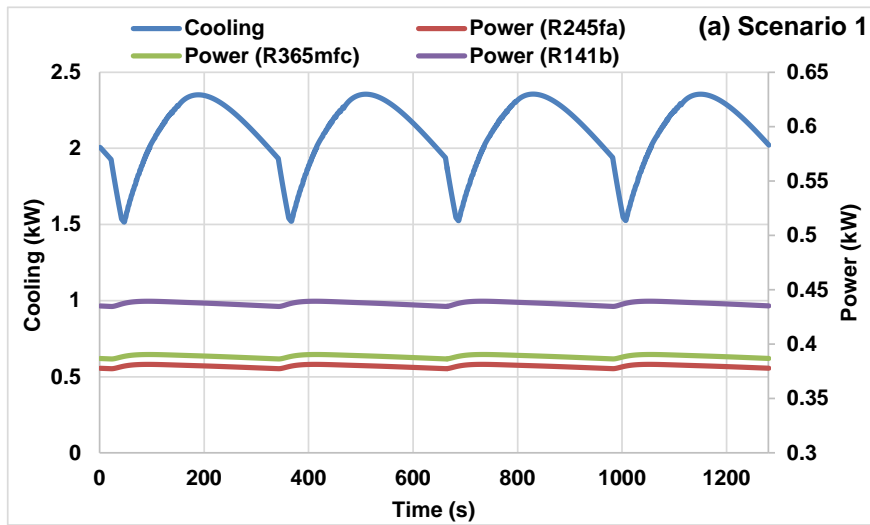
328

329
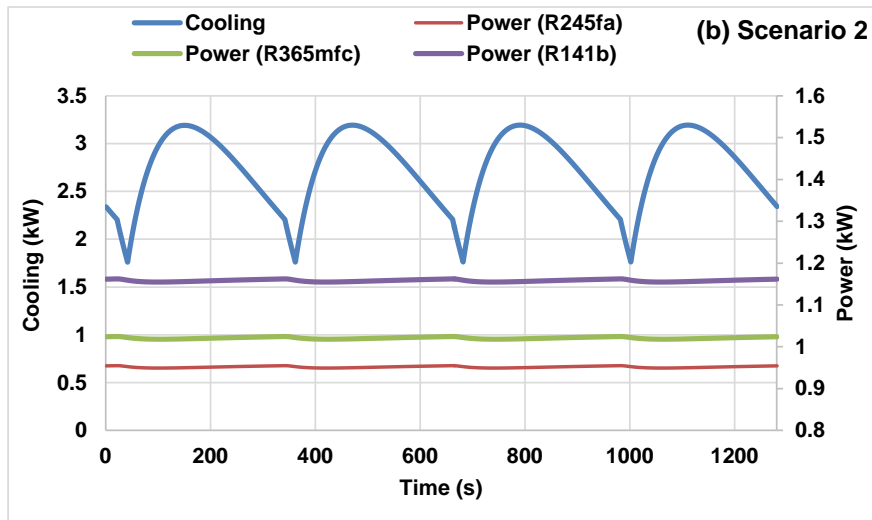
330
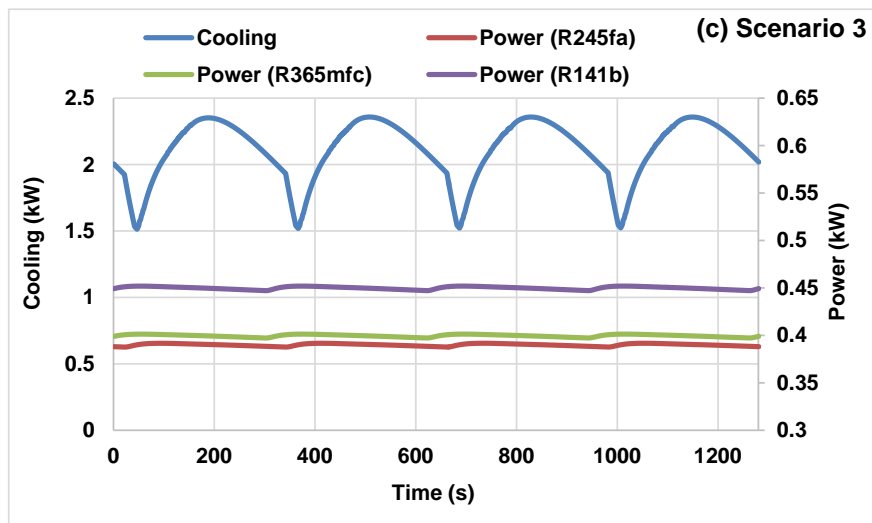
331
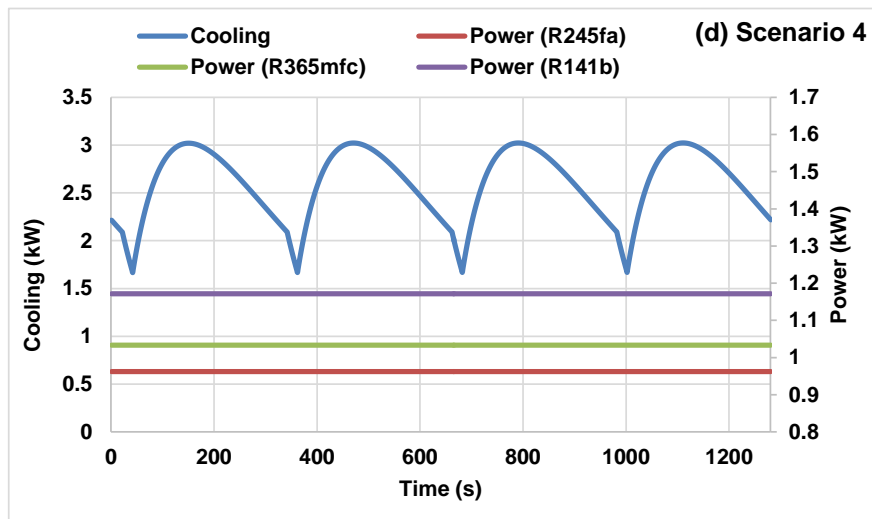
332 **Figure 8: Cooling and power generating using SAPO-34/water with heat source temperature of 95 ^{o}C .**

333

334

(a) R245fa

335

(b) R365mfc

336

(c) R141b
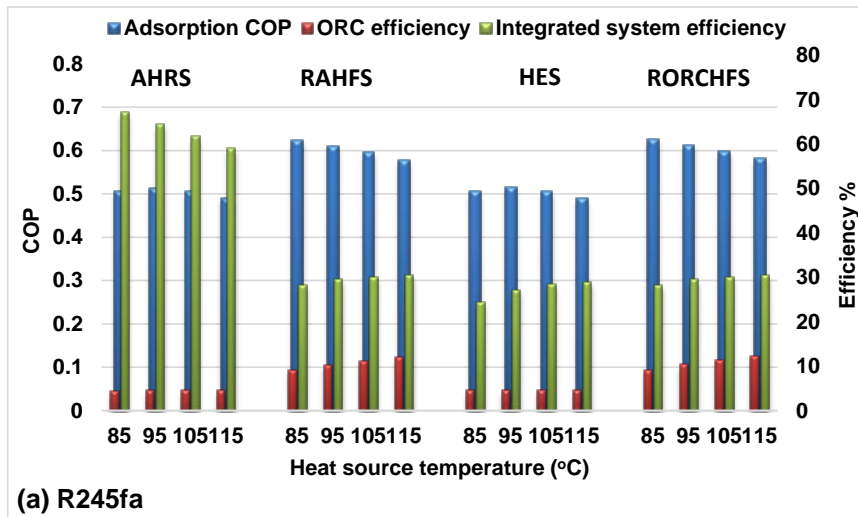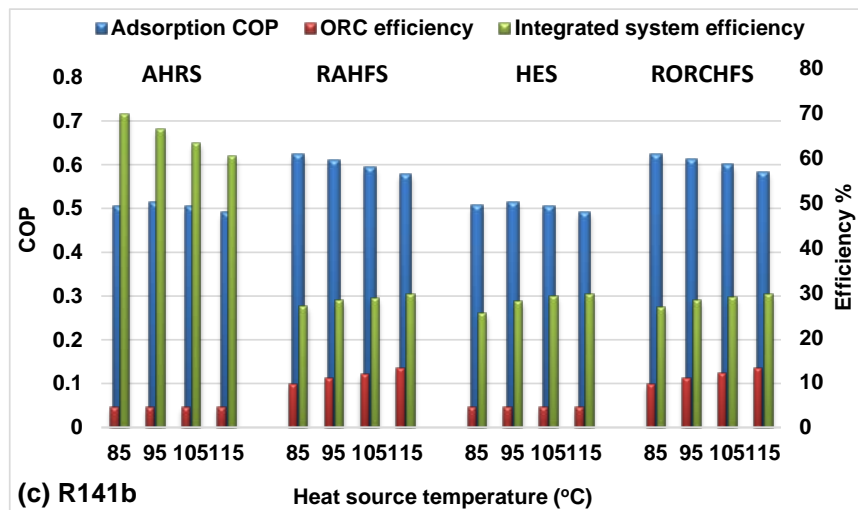
337

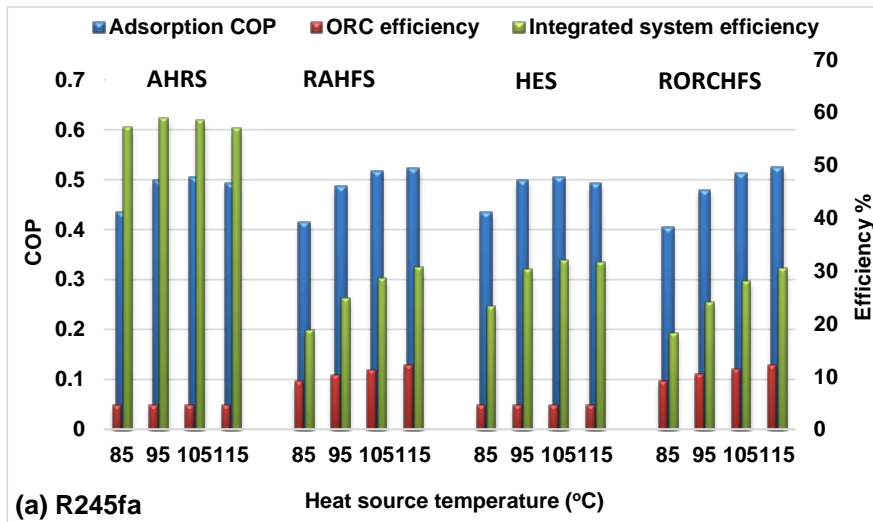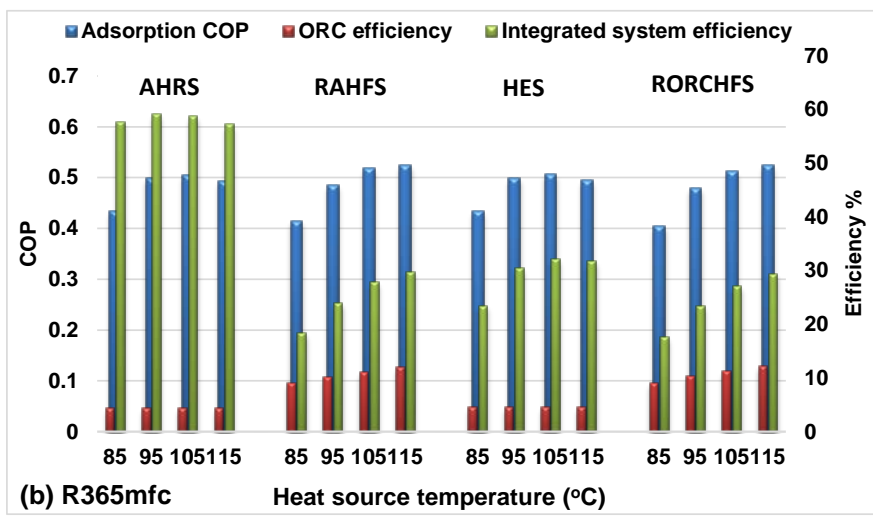**Figure 9: Effect of using the four scenarios on COP and system efficiencies utilising silica-gel/water.**
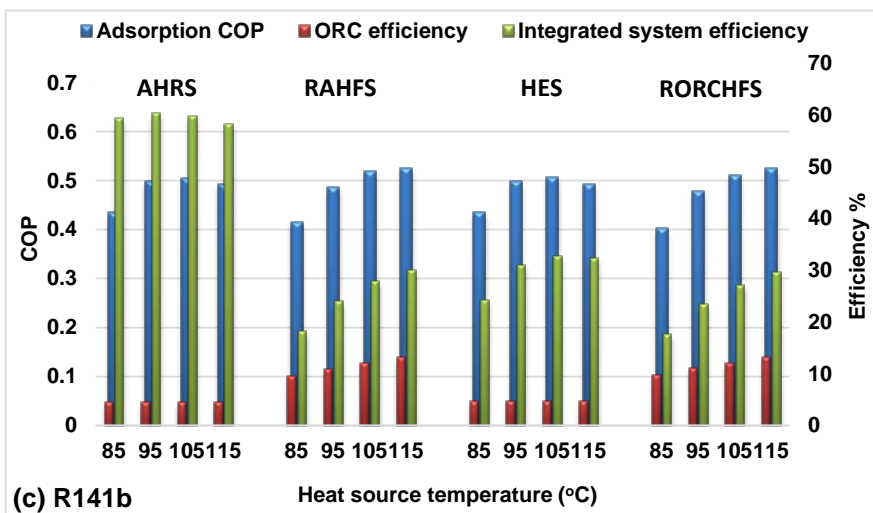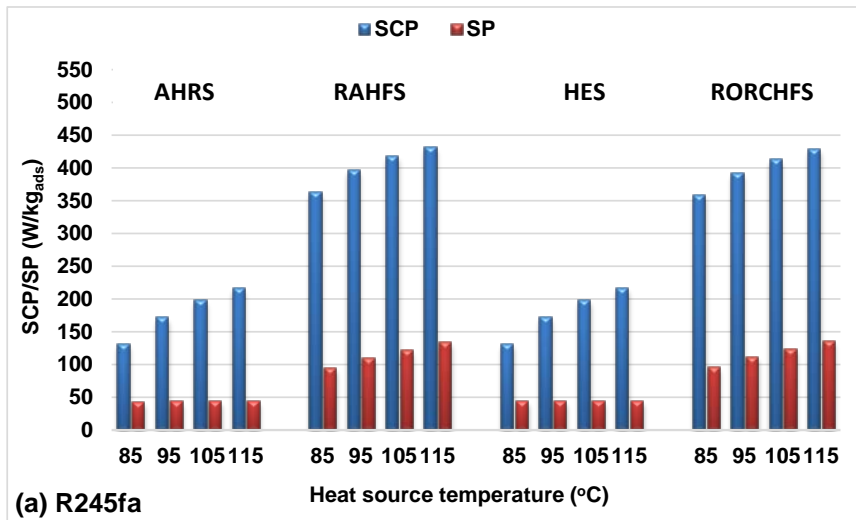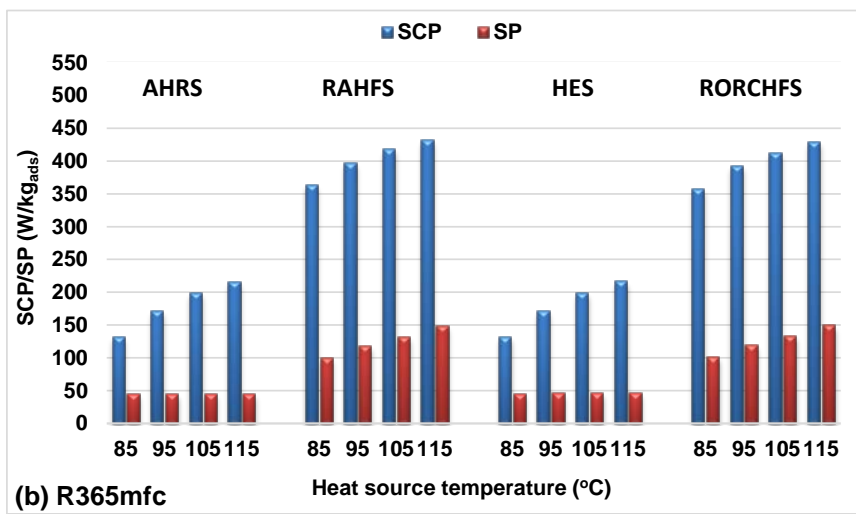
338

339

340

341

342   **Figure 10: Effect of using the four scenarios on COP and system efficiencies utilising SAPO-34/water.**
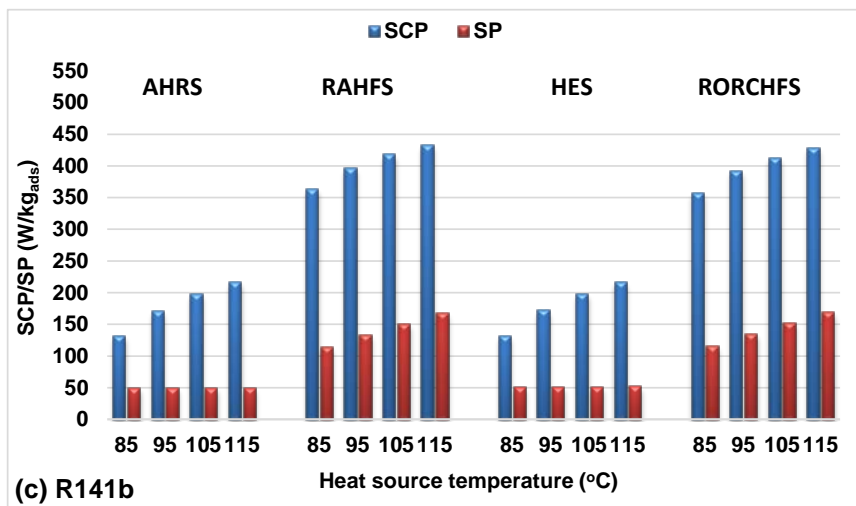
343

(a) R245fa

344

(b) R365mfc

345

(c) R141b

346   **Figure 11: Effect of using the four scenarios on the SCP and SP utilising silica-gel/water.**

22

(a) R245fa

(b) R365mfc

(c) R141b
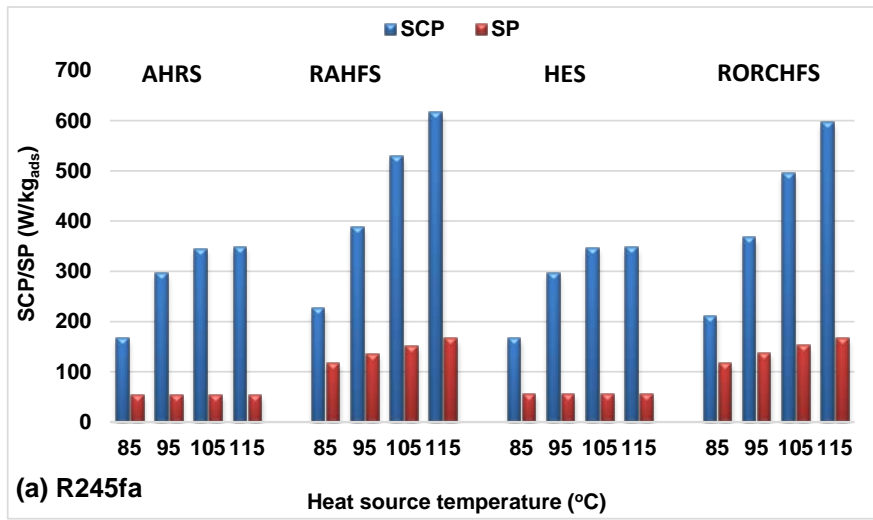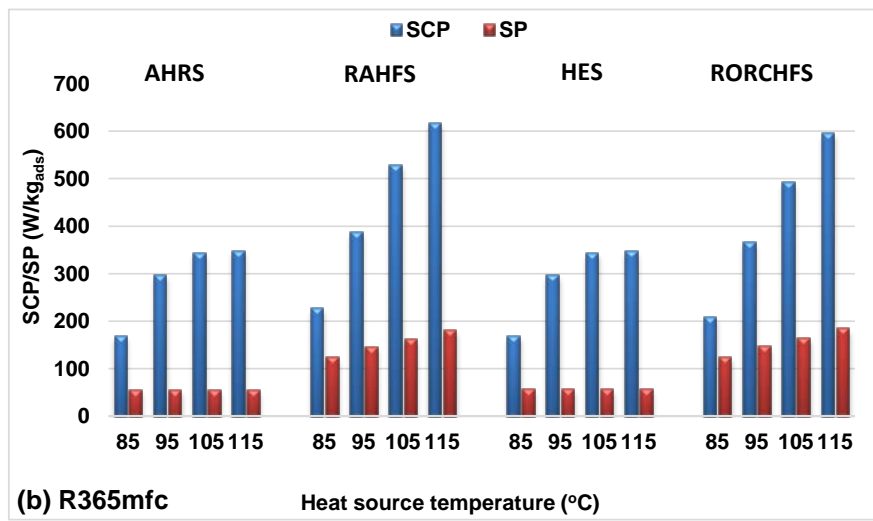
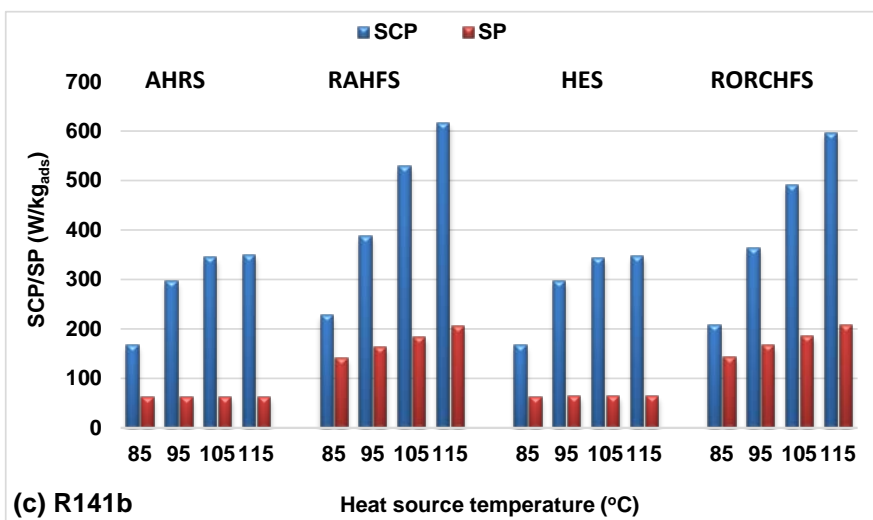**Figure 12: Effect of using the four scenarios on the SCP and SP utilising SAPO-34/water.**

6. Conclusion

A two-bed adsorption cooling system has been integrated with an Organic Rankine cycle (ORC) to generate cooling and electricity simultaneously using four different scenarios. In the first three scenarios, adsorption system is set up as a topping system, while ORC is set up as a bottoming system. The first scenario AHRS, the adsorption heat is recovered from the adsorption bed and used to power the ORC system, and in this case, no additional heat is applied. The second scenario RAHFS, the heating fluid leaving the adsorption system is used to power the ORC system. In the third scenario HES, a heat exchanged is used to add more heat from the heating source to the cooling line leaving the adsorption system to enhance the performance of the ORC. In the fourth scenario RORCHFS, the ORC system is set as a topping system, while the adsorption system is set as a bottoming system and the adsorption system is powered using the heating fluid leaving the ORC system.. AQSOA-ZO2 (SAPO-34)/water and silica-gel/water have been used as adsorption working pairs, while R245fa, R365mfc and R141b have been used as an ORC working fluids. The main results of this investigation can be surmised as:

1. Integrating adsorption cooling system with ORC offers the advantage of generating cooling and power simultaneously and it can improve the overall system efficiency.

2. The four proposed scenarios offer wide-range options for energy designers and customers to use localised cooling and power generation units that utilize low grade heat sources.

3. AHRS achieved the maximum integrated system efficiency of 60% utilizing SAPO-34/water and R141b and 70% utilizing silica-gel/water and R141b.

4. RAHFS and RORCHFS achieved the maximum COP of about 0.63 and 0.53 using silica gel and SAPO-34 respectively.

5. Utilizing SAPO-34 and R141b in RORCHFS achieved the maximum specific power of 208 W/kg_{ads}, while in RAHFS they achieved the maximum specific cooling power of 616 W/kg_{ads}.

6. Using heat exchanger in HES can slightly increase the ORC efficiency and SP, but decrease the integrated system efficiency compared to AHRS because of using additional heat.

24

382 **References**

383 [1] S. M. Moosavian, N. A. Rahim, J. Selvaraj, and K. H. Solangi, "Energy policy to
384   promote photovoltaic generation," *Renew. Sustain. Energy Rev.*, vol. 25, pp. 44–58,
385   2013.

386 [2] T. C. Hung, T. Y. Shai, and S. K. Wang, "A review of organic rankine cycles (ORCs)
387   for the recovery of low-grade waste heat," *Energy*, vol. 22, no. 7, pp. 661–667, 1997.

388 [3] R. Rayegan and Y. X. Tao, "A procedure to select working fluids for Solar Organic
389   Rankine Cycles (ORCs)," *Renew. Energy*, vol. 36, no. 2, pp. 659–670, 2011.

390 [4] F. A. Al-Sulaiman, F. Hamdullahpur, and I. Dincer, "Greenhouse gas emission and
391   exergy assessments of an integrated organic Rankine cycle with a biomass combustor
392   for combined cooling, heating and power production," *Appl. Therm. Eng.*, vol. 31, no.
393   4, pp. 439–446, 2011.

394 [5] T. Guo, H. X. Wang, and S. J. Zhang, "Fluids and parameters optimization for a novel
395   cogeneration system driven by low-temperature geothermal sources," *Energy*, vol. 36,
396   no. 5, pp. 2639–2649, 2011.

397 [6] V. L. Le, M. Feidt, A. Kheiri, and S. Pelloux-Prayer, "Performance optimization of
398   low-temperature power generation by supercritical ORCs (organic Rankine cycles)
399   using low GWP (global warming potential) working fluids," *Energy*, vol. 67, pp. 513–
400   526, 2014.

401 [7] G. Pei, J. Li, and J. Ji, "Analysis of low temperature solar thermal electric generation
402   using regenerative Organic Rankine Cycle," *Appl. Therm. Eng.*, vol. 30, no. 8–9, pp.
403   998–1004, 2010.

404 [8] P. J. Mago, L. M. Chamra, K. Srinivasan, and C. Somayaji, "An examination of
405   regenerative organic Rankine cycles using dry fluids," *Appl. Therm. Eng.*, vol. 28, no.
406   8–9, pp. 998–1007, 2008.

407 [9] I. H. Aljundi, "Effect of dry hydrocarbons and critical point temperature on the
408   efficiencies of organic Rankine cycle," *Renew. Energy*, vol. 36, no. 4, pp. 1196–1202,
409   2011.

410 [10] B. F. Tchanche, G. Papadakis, G. Lambrinos, and A. Frangoudakis, "Fluid selection
411   for a low-temperature solar organic Rankine cycle," *Appl. Therm. Eng.*, vol. 29, no.
412   11–12, pp. 2468–2476, 2009.

413 [11] J. P. Roy, M. K. Mishra, and A. Misra, "Performance analysis of an Organic Rankine
414   Cycle with superheating under different heat source temperature conditions," *Appl.
415   Energy*, vol. 88, no. 9, pp. 2995–3004, 2011.

416 [12] F. Asdrubali and S. Grignaffini, "Experimental evaluation of the performances of a
417   H2O-LiBr absorption refrigerator under different service conditions," *Int. J. Refrig.*,
418   vol. 28, no. 4, pp. 489–497, 2005.

419 [13] G. A. Florides, S. A. Kalogirou, S. A. Tassou, and L. C. Wrobel, "Design and
420   construction of a LiBr-water absorption machine," *Energy Convers. Manag.*, vol. 44,
421   no. 15, pp. 2483–2508, 2003.

422 [14] N. D. Banker, M. Prasad, P. Dutta, and K. Srinivasan, "Activated carbon + HFC 134a
423   based two stage thermal compression adsorption refrigeration using low grade thermal
424   energy sources," *Appl. Therm. Eng.*, vol. 29, no. 11–12, pp. 2257–2264, 2009.

425 [15] M. Z. I. Khan, K. C. A. Alam, B. B. Saha, A. Akisawa, and T. Kashiwagi, "Study on a

re-heat two-stage adsorption chiller - The influence of thermal capacitance ratio, overall thermal conductance ratio and adsorbent mass on system performance," *Appl. Therm. Eng.*, vol. 27, no. 10, pp. 1677–1685, 2007.

[16] A. S. Uyun, A. Akisawa, T. Miyazaki, Y. Ueda, and T. Kashiwagi, "Numerical analysis of an advanced three-bed mass recovery adsorption refrigeration cycle," *Appl. Therm. Eng.*, vol. 29, no. 14–15, pp. 2876–2884, Oct. 2009.

[17] W. S. Loh, I. I. El-Sharkawy, K. C. Ng, and B. B. Saha, "Adsorption cooling cycles for alternative adsorbent/adsorbate pairs working at partial vacuum and pressurized conditions," *Appl. Therm. Eng.*, vol. 29, no. 4, pp. 793–798, 2009.

[18] L. W. Wang, R. Z. Wang, and R. G. Oliveira, "A review on adsorption working pairs for refrigeration," *Renew. Sustain. Energy Rev.*, vol. 13, no. 3, pp. 518–534, 2009.

[19] X. Wang and H. T. Chua, "Two bed silica gel–water adsorption chillers: An effectual lumped parameter model," *Int. J. Refrig.*, vol. 30, no. 8, pp. 1417–1426, Dec. 2007.

[20] H. T. Chua, K. C. Ng, W. Wang, C. Yap, and X. L. Wang, "Transient modeling of a two-bed silica gel–water adsorption chiller," *Int. J. Heat Mass Transf.*, vol. 47, no. 4, pp. 659–669, Feb. 2004.

[21] W. Chang, C. Wang, and C. Shieh, "Experimental study of a solid adsorption cooling system using flat-tube heat exchangers as adsorption bed," *Appl. Therm. Eng.*, vol. 27, pp. 2195–2199, 2007.

[22] S. Vijayaraghavan and D. Y. Goswami, "A combined power and cooling cycle modified to improve resource utilization efficiency using a distillation stage," *Energy*, vol. 31, no. 8–9, pp. 1177–1196, 2006.

[23] A. A. Hassan, Y. Goswami, and S. Vijayaraghavan, "First and Second Law Analysis of a New Power and Refrigeration Thermodynamic Cycle Using a Solar Heat Source," *Sol. Energy*, vol. 73, no. 5, pp. 385–393, 2003.

[24] M. Liu and N. Zhang, "Proposal and analysis of a novel ammonia-water cycle for power and refrigeration cogeneration," *Energy*, vol. 32, no. 6, pp. 961–970, 2007.

[25] D. Zheng, B. Chen, Y. Qi, and H. Jin, "Thermodynamic analysis of a novel absorption power/cooling combined-cycle," *Appl. Energy*, vol. 83, no. 4, pp. 311–323, 2006.

[26] N. Zhang and N. Lior, "Development of a Novel Combined Absorption Cycle for Power Generation and Refrigeration," *J. Energy Resour. Technol.*, vol. 129, no. 3, p. 254, 2007.

[27] Y. Lu, H. Bao, Y. Yuan, Y. Wang, L. Wang, and A. P. Roskilly, "Optimisation of a novel resorption cogeneration using mass and heat recovery," *Energy Procedia*, vol. 61, pp. 1103–1106, 2014.

[28] L. Jiang, L. W. Wang, A. P. Roskilly, and R. Z. Wang, "Design and performance analysis of a resorption cogeneration system," *Int. J. Low-Carbon Technol.*, vol. 8, no. SUPPL1, pp. 85–91, 2013.

[29] L. Wang, F. Ziegler, A. P. Roskilly, R. Wang, and Y. Wang, "A resorption cycle for the cogeneration of electricity and refrigeration," *Appl. Energy*, vol. 106, pp. 56–64, 2013.

[30] H. Bao, Y. Wang, and A. P. Roskilly, "Modelling of a chemisorption refrigeration and power cogeneration system," *Appl. Energy*, vol. 119, pp. 351–362, 2014.

[31] H. Bao, Y. Wang, C. Charalambous, Z. Lu, L. Wang, R. Wang, and A. P. Roskilly,

"Chemisorption cooling and electric power cogeneration system driven by low grade heat," *Energy*, vol. 72, pp. 590–598, 2014.

[32] L. Jiang, L. W. Wang, X. F. Zhang, C. Z. Liu, and R. Z. Wang, "Performance prediction on a resorption cogeneration cycle for power and refrigeration with energy storage," *Renew. Energy*, vol. 83, pp. 1250–1259, 2015.

[33] Y. Lu, Y. Wang, H. Bao, Y. Yuan, L. Wang, and A. P. Roskilly, "Analysis of an optimal resorption cogeneration using mass and heat recovery processes," *Appl. Energy*, vol. 160, pp. 892–901, 2015.

[34] F. Al-mousawi, R. Al-dadah, and S. Mahmoud, "MIL101Cr MOF – Water Adsorption System for Cooling and Power Generation Using Waste Heat," SusTEM2015 Conference Proceedings, pp. 291–301, 2015. Avialble online at http://research.ncl.ac.uk/sustem/sustem2015conference/proceedings/

[35] F. N. Al-Mousawi, R. Al-Dadah, and S. Mahmoud, "Low grade heat driven adsorption system for cooling and power generation with small-scale radial inflow turbine" *Appl. Energy*, vol. 183, pp. 1302–1316, 2016.

[36] F. N. Al-Mousawi, R. Al-Dadah, and S. Mahmoud, "Low grade heat driven adsorption system for cooling and power generation using advanced adsorbent materials," *Energy Convers. Manag.*, vol. 126, pp. 373–384, 2016.

[37] L. Jiang, L. Wang, R. Wang, P. Gao, and F. Song, "Investigation on cascading cogeneration system of ORC (Organic Rankine Cycle) and CaCl2/BaCl2 two-stage adsorption freezer," *Energy*, vol. 71, pp. 377–387, 2014.

[38] L. Wang, A. P. Roskilly, R. Wang, P. Taylor, "Solar Powered Cascading Cogeneration Cycle with ORC and Adsorption Technology for Electricity and Refrigeration," *Heat Transf. Eng.*, vol. 35, no. 11–12, pp. 1028–1034, 2014.

[39] X. Wang, H. T. Chua, and K. C. Ng, "Experimental investigation of silica gel-water adsorption chillers with and without a passive heat recovery scheme," *Int. J. Refrig.*, vol. 28, no. 5, pp. 756–765, 2005.

[40] Q. W. Pan, R. Z. Wang, and L. W. Wang, "Comparison of different kinds of heat recoveries applied in adsorption refrigeration system," *Int. J. Refrig.*, vol. 55, pp. 37–48, 2015.

[41] K. C. Leong and Y. Liu, "Numerical study of a combined heat and mass recovery adsorption cooling cycle," *Int. J. Heat Mass Transf.*, vol. 47, no. 22, pp. 4761–4770, 2004.

[42] MITSUBISHI PLASTICS, Zeolite, AQSOA, https://www.mpi.co.jp/english/products/industrial_materials/im010.html

[43] B. Sun and A. Chakraborty, "Thermodynamic formalism of water uptakes on solid porous adsorbents for adsorption cooling applications," APPLIED PHYSICS LETTERS vol.104, 201901, 2014. vol. 201901, 2014.

[44] T. Miyazaki, A. Akisawa, B. B. Saha, I. I. El-Sharkawy, and A. Chakraborty, "A new cycle time allocation for enhancing the performance of two-bed adsorption chillers," *Int. J. Refrig.*, vol. 32, no. 5, pp. 846–853, 2009.

[45] B. B. Saha, S. Koyama, T. Kashiwagi, A. Akisawa, K. C. Ng, and H. T. Chua, "Waste heat driven dual-mode, multi-stage, multi-bed regenerative adsorption system," *Int. J. Refrig.*, vol. 26, no. 7, pp. 749–757, 2003.

[46] I. I. El-Sharkawy, H. Abdelmeguid, and B. B. Saha, "Towards an optimal performance of adsorption chillers: Reallocation of adsorption/desorption cycle times," *Int. J. Heat Mass Transf.*, vol. 63, pp. 171–182, 2013.

[47] H. Z. Hassan, A. A. Mohamad, Y. Alyousef, and H. A. Al-ansary, "A review on the equations of state for the working pairs used in adsorption cooling systems," *Renew. Sustain. Energy Rev.*, vol. 45, pp. 600–609, 2015.

[48] A. Sadeghlu, M. Yari, S. M. S. Mahmoudi, and H. B. Dizaji, "Performance evaluation of Zeolite 13X/CaCl2 two-bed adsorption refrigeration system," *Int. J. Therm. Sci.*, vol. 80, no. 1, pp. 76–82, 2014.

[49] P. G. Youssef, S. M. Mahmoud, and R. K. AL-Dadah, "Performance analysis of four bed adsorption water desalination/refrigeration system, comparison of AQSOA-Z02 to silica-gel," *Desalination*, vol. 375, pp. 100–107, 2015.

[50] B. B. Saha, E. C. Boelman, and T. Kashiwagi, "Computational analysis of an advanced adsorption-refrigeration cycle," *Energy*, vol. 20, no. 10, pp. 983–994, 1995.

[51] C. Y. Tso, C. Y. H. Chao, and S. C. Fu, "Performance analysis of a waste heat driven activated carbon based composite adsorbent - Water adsorption chiller using simulation model," *Int. J. Heat Mass Transf.*, vol. 55, no. 25–26, pp. 7596–7610, 2012.

[52] S. K. Farid, M. M. Billah, M. Z. I. Khan, M. M. Rahman, and U. M. Sharif, "A numerical analysis of cooling water temperature of two-stage adsorption chiller along with different mass ratios," *Int. Commun. Heat Mass Transf.*, vol. 38, no. 8, pp. 1086–1092, 2011.

[53] S. Safarian and F. Aramoun, "Energy and exergy assessments of modified Organic Rankine Cycles (ORCs)," *Energy Reports*, vol. 1, pp. 1–7, 2015.

[54] P. Collings, Z. Yu, and E. Wang, "A dynamic organic Rankine cycle using a zeotropic mixture as the working fluid with composition tuning to match changing ambient conditions," *Appl. Energy*, vol. 171, pp. 581–591, 2016.

[55] K. Rahbar, S. Mahmoud, R. K. Al-dadah, and N. Moazami, "Modelling and optimization of organic Rankine cycle based on a small-scale radial inflow turbine," *Energy Convers. Manag.*, vol. 91, pp. 186–198, 2015.

[56] B. Shi, R. Al-Dadah, S. Mahmoud, A. Elsayed, and E. Elsayed, "CPO-27(Ni) metal-organic framework based adsorption system for automotive air conditioning," *Appl. Therm. Eng.*, vol. 106, pp. 325–333, 2016.